

1 Research article

2

3

4

5 **Light-dependent induction of *Edn2* expression and attenuation of retinal pathology by**
6 **endothelin receptor antagonists in *Prominin-1*- deficient mice**

7

8

9

10 Yuka Kobayashi¹, Shizuka Watanabe², Manabu Shirai³, Chiemi Yamashiro¹, Tadahiko Ogata¹,
11 Fumiaki Higashijima¹, Takuya Yoshimoto¹, Takahide Hayano⁴, Yoshiyuki Asai⁴,
12 Noriaki Sasai^{2,5,*} and Kazuhiro Kimura^{1,5,*}

13

14

15

16 ¹Department of Ophthalmology, Yamaguchi University Graduate School of Medicine, 1-1-1 Minami-
17 kogushi, Ube 755-0046, Japan

18 ²Developmental Biomedical Science, Division of Biological Sciences, Nara Institute of Science and
19 Technology, 8916-5 Takayama-cho, Ikoma 630-0192, Japan

20 ³Omics Research Center (ORC), National Cerebral and Cardiovascular Center, 6-1 Kishibe Shinmachi,
21 Suita, Osaka 564-8565, Japan

22 ⁴Department of Systems Bioinformatics, Yamaguchi University Graduate School of Medicine, 1-1-1
23 Minami-kogushi, Ube 755-0046, Japan

24 ⁵ Co-senior authors

25

26

27

28 ***Address for correspondence:**

29 Kazuhiro Kimura (e-mail: k.kimura@yamaguchi-u.ac.jp) or

30 Noriaki Sasai (e-mail: noriakisasai@bs.naist.jp)

31

32 **Running Title**

33 Blocking endothelin relieves retinopathy

34 **Abstract**

35 Retinitis pigmentosa (RP) and macular dystrophy (MD) are prevalent retinal degenerative diseases
36 associated with gradual photoreceptor death. These diseases are often caused by genetic mutations that
37 result in degeneration of the retina postnatally after it has fully developed. The *Prominin-1* gene (*Prom1*)
38 is a causative gene for RP and MD, and *Prom1*- knockout (KO) mice recapitulate key features of these
39 diseases including light-dependent retinal degeneration and stenosis of retinal blood vessels. The
40 mechanisms underlying progression of such degeneration have remained unknown, however. We here
41 analysed early events associated with retinal degeneration in *Prom1*-KO mice. We found that
42 photoreceptor cell death and glial cell activation occur between 2 and 3 weeks after birth. High-throughput
43 analysis revealed that expression of the endothelin-2 gene (*Edn2*) was markedly up-regulated in the
44 *Prom1*-deficient retina during this period. Expression of *Edn2* was also induced by light stimulation in
45 *Prom1*-KO mice that had been reared in the dark. Finally, treatment with endothelin receptor antagonists
46 attenuated photoreceptor cell death, gliosis, and retinal vessel stenosis in *Prom1*-KO mice. Our findings
47 suggest that inhibitors of endothelin signalling may delay the progression of RP and MD and therefore
48 warrant further study as potential therapeutic agents for these diseases.

49

50 **Keywords**

51 prominin-1, photoreceptor, glial cell, retinal degeneration, endothelin-2, endothelin receptor antagonists

52 **1. Introduction**

53 Both retinitis pigmentosa (RP) and macular dystrophy (MD) are inherited retinal disorders
54 associated with progressive photoreceptor cell death [1]. These diseases have a combined prevalence of 1
55 in 3000 to 4000 people worldwide. Initial symptoms include nyctalopia (night blindness) and visual field
56 deficits, which are followed by loss of visual acuity and colour blindness and eventually by complete
57 blindness. Although >60 genes encoding various types of protein - including membrane proteins,
58 transcription factors, splicing regulators, and enzymes related to the visual cycle - have been implicated in
59 RP and MD [1], these conditions remain incurable, with effective therapeutic strategies remaining to be
60 established, and they have profound effects on the quality of life.

61 The *Prominin-1* gene (*Prom1*, also known as *AC133*, *CD133*, and *RP41*) encodes a pentaspan
62 transmembrane glycoprotein that is expressed in photoreceptor cells of the retina as well as in kidney and
63 testis [2]. Several mutations of *Prom1* have been identified in individuals with RP or MD [3-5], with all
64 such mutations resulting in amino acid substitutions or carboxyl-terminal truncations of the encoded
65 protein. The mechanisms underlying RP and MD associated with *Prom1* mutations have been investigated
66 by studies of several lines of *Prom1*-knockout (KO) mice [5-7]. Although photoreceptor cells develop
67 normally in these KO mice, they begin to degenerate after birth, resulting in a progressive loss of the outer
68 nuclear layer (ONL) of the retina and recapitulation of the signs of RP and MD. The retinal vasculature
69 also becomes attenuated with disease progression [7].

70 We previously showed that photoreceptor cells of the *Prom1*-KO mouse retina degenerate in
71 response to light stimulation. Such mice reared in a completely dark setting thus manifested a marked
72 delay in the loss of photoreceptor cells. We therefore suggested that the mutant retinal cells are
73 hypersensitive to light stimulation and experience phototoxicity [6]. The visual cycle was also found to be
74 impaired in the *Prom1*-KO cells, and treatment based on chemical compounds that modulate the visual
75 cycle was found to mitigate the mutant phenotype [6].

76 The *Prom1* protein localises to the connecting cilium and outer segment of both rod and cone
77 photoreceptors [3]. Ultrastructural analysis revealed the structure of the outer segment to be severely
78 disorganised in photoreceptor cells of *Prom1*-KO mice, whereas other photoreceptor components -
79 including the inner segment, nucleus, and axon - remained largely intact [6, 7]. Biochemical analysis has
80 shown that two tyrosine residues in the carboxyl-terminal region of *Prom1* are phosphorylated by the
81 tyrosine kinases *Src* and *Fyn*, although the physiological implications of such phosphorylation remain to
82 be elucidated [8]. *Prom1* has also been shown to interact with the p85 regulatory subunit of
83 phosphatidylinositol 3-kinase (PI3K) and to be essential for both the self-renewal and tumourigenic
84 capacity of glioma stem cells [9]. In addition, *Prom1* has been detected in cilia, which are protrusive
85 structures at the cell membrane and key signalling hubs [10], and to be essential for maximisation of
86 Hedgehog signalling in neural stem cells [11]. We recently showed that *Prom1* activates the small GTPase
87 Rho and regulates chloride conductance triggered by intracellular calcium uptake [12].

88 To characterise the mechanisms underlying the role of Prom1 dysfunction in retinal degeneration
89 and thereby to provide insight into potential treatments for *Prom1* mutation-associated RP and MD, we
90 here investigated the initial manifestations of such degeneration. We analysed *Prom1* expression as well
91 as the ONL transition in *Prom1*-KO mice. We then performed a high-throughput expression analysis to
92 identify genes responsible for degeneration of the *Prom1*-deficient retina. Our results implicated an
93 inflammatory pathway dependent on the endothelin 2 gene (*Edn2*), and we found that a chemical
94 treatment targeted to endothelin signalling mitigated the deterioration of retinal structure and function in
95 *Prom1*-KO mice.

96

97 **2. Methods**

98 **2.1. Mice**

99 *Prom1*-KO mice were established previously (CDB0623K, <http://www2.clst.riken.jp/arg/methods.html>),
100 and they were reared on a hybrid genetic background of C57BL/6 and CBA/NSlc strains. The targeting
101 vector for *Prom1* ablation contained the *lacZ* (β -galactosidase) gene, with the result that expression of this
102 latter gene reflects that of *Prom1*. Both the *Prom1*-KO mice and their wild-type (WT) littermates were
103 kept on a 12-hour-light, 12-hour-dark cycle, with the cage racks being covered with blackout curtains and
104 all procedures including feeding and cage maintenance being performed in the absence of light (<0.5 lux)
105 during the dark phase. For experiments involving light stimulation, mice were exposed for 3 h to a light
106 panel (LED viewer 5000; Shinko, Tokyo, Japan) placed on top of the cage, which resulted in a light
107 intensity of 3800 lux at the bottom of the cage. For chemical treatment, mice received intraperitoneal
108 injections (2 mg/kg) of each of the endothelin receptor antagonists BQ-123 (ab141005, Abcam) and BQ-
109 788 (ab144504, Abcam) on postnatal day (P) 14, P19, and P24. The mice were then subjected to analysis
110 on P28.

111

112 **2.2. RNA extraction and RT-qPCR analysis**

113 The retina, retinal pigment epithelium (RPE), and testis were dissected from mice killed by cervical
114 dislocation. Total RNA was extracted from the isolated tissue and was subjected to reverse transcription
115 (RT) with the use of a NucleoSpin RNA extraction kit (U955C, Takara) and PrimeScript RT reagent kit
116 (RR037, Takara), respectively. The resulting cDNA was subjected to quantitative polymerase chain
117 reaction (qPCR) analysis with a CFX qPCR machine (Bio-Rad) and with primers listed in supplementary
118 table S1. The amplification data were analysed with the comparative C_t method, and gene expression
119 levels were normalised by that of the glyceraldehyde-3-phosphate dehydrogenase gene (*Gapdh*).

120

121 **2.3. High-throughput expression analysis**

122 Total RNA samples were prepared from three (P14) or four (P21) retinas of WT or *Prom1*-KO mice and
123 were used to synthesise cDNA libraries with a TruSeq stranded-mRNA library preparation kit (Illumina,
124 20020594). The libraries were sequenced with the NextSeq 500 platform (Illumina). In total,
125 approximately twenty million reads/sample were mapped with the CLC genomics workbench software
126 (Qiagen) [13]. The sequencing data were deposited in the DNA Data Bank of Japan (DDBJ) public
127 database, with the accession number of SSUB016168. Gene ontology (GO) term analysis was performed
128 according to the Kyoto Encyclopaedia of Genes and Genomes database (KEGG,
129 <https://www.genome.jp/kegg>).

130

131 **2.4. Immunofluorescence analysis, β -galactosidase and isolectin staining, and TUNEL analysis**

132 For immunofluorescence analysis, the enucleated retina was fixed for 2 h with a mixture of 1%
133 paraformaldehyde and 0.2% glutaraldehyde in phosphate-buffered saline (PBS), incubated overnight in
134 PBS containing 15% sucrose, embedded in O.C.T. compound (Sakura), and sectioned at a thickness of 12
135 μm . The sections were exposed to mouse monoclonal antibodies to GFAP (G3893; Sigma) or rabbit
136 polyclonal antibodies to Iba-1 (019-19741; Wako), and immune complexes were detected with Cy3-
137 conjugated secondary antibodies (715-166-151 and 715-166-152 for mouse and rabbit, respectively;
138 Jackson Immunoresearch). Nuclei were counterstained with 4',6-diamidino-2-phenylindole (DAPI) with
139 the use of DAPI Fluoromount-G (0100-20; Southern Biotech). Sections were also stained for β -
140 galactosidase (β -gal) activity with the use of a staining kit (11828673001, Roche). Apoptotic cells were
141 detected by TUNEL analysis with digoxigenin-labelled dUTP (S7105, Merck Millipore), terminal
142 deoxynucleotidyl transferase (3333566001, Merck), and rhodamine-conjugated antibodies to digoxigenin
143 (11207750910, Roche). For preparation of flat-mount samples, the retina was fixed for 150 min with 4%
144 paraformaldehyde and the RPE was peeled off. The samples were subjected to isolectin staining by
145 consecutive exposure to 5% dried skim milk and Alexa Flour 488-conjugated GS-IB4 (I21411, Thermo
146 Fisher Scientific) as described previously [14]. Images were acquired with an LSM 710 confocal
147 microscope (Zeiss) for immunofluorescence, β -gal, and TUNEL staining, or with a BZ-X710 microscope
148 (Keyence) for flat-mount preparations. Imaging data were processed and integrated with Photoshop
149 (Adobe) and Illustrator (Adobe) software, respectively.

150

151 **2.5. Statistical analysis**

152 Quantitative data are presented as means \pm s.e.m. Differences between two or among more than two
153 groups were evaluated with the two-tailed Student's *t* test and by one-way analysis of variance (ANOVA)
154 followed by Tukey's post hoc test, respectively. Statistical analysis was performed with Prism software
155 (Graphpad), and a *p* value of <0.05 was considered statistically significant.

156

157 **3. Results**

158 **3.1. *Prom1* is expressed in the retina from perinatal to adult stages**

159 We previously showed that retinal cells in *Prom1*-KO mice appear to develop normally before the onset of
160 degeneration [6]. We here first examined the spatiotemporal expression of *Prom1* in the mouse retina.
161 Given that our *Prom1*-KO mice harbour the *lacZ* gene at the *Prom1* locus, we performed staining for β -
162 gal activity in the heterozygous mutant mice at birth as well as at P2 (figure 1a-a’'), P14 (figure 1b-b’'),
163 P21 (figure 1c-c’'), and P42 (figure 1d-d’'). At all the stages analysed, β -gal staining was localised
164 predominantly to the outer layers in the retina, with more sporadic staining also apparent in the inner
165 nuclear layer (INL). Given that retinal phenotypes of *Prom1*-KO mice are not obvious until 2 weeks after
166 birth, these results suggested that *Prom1* expression precedes the onset of function of the encoded protein
167 in postnatal retinal homeostasis.

168

169 **3.2. The *Prom1*-KO mouse retina manifests both apoptosis and an inflammatory response at 3** 170 **weeks after birth**

171 We previously showed that the retina of *Prom1*-KO mice appears normal at P14 and begins to
172 degenerate soon after the animals first open their eyes at P14 [6]. We therefore investigated whether the
173 *Prom1*-deficient retina might undergo apoptosis in response to light exposure. Whereas the TUNEL assay
174 revealed few apoptotic cells in the retina of WT or *Prom1*-KO mice at P14 (figure 2a and b), a significant
175 increase in the number of TUNEL-positive cells, located mainly in the ONL, was detected at P21 in the
176 *Prom1*-KO retina (figure 2c-e). These results suggested that programmed cell death by apoptosis begins
177 to occur in the ONL of the retina between 2 and 3 weeks after birth in *Prom1*-KO mice.

178 Glial fibrillary acidic protein (GFAP) is an intermediate filament protein that is expressed by
179 Müller glia in response to retinal injury [15, 16]. Similarly, Iba-1 is a scaffold protein that is expressed in
180 microglia and which is up-regulated during an inflammatory response [17, 18]. We therefore next
181 examined whether the *Prom1*-KO retina might undergo light-induced inflammation by analysing the
182 expression of these two proteins. Immunofluorescence analysis revealed that, whereas both GFAP and
183 Iba-1 were essentially undetectable in the WT or *Prom1*-KO retina at P14 (figure 2f-i), a marked increase
184 in the extent of staining for both proteins was observed in the *Prom1*-KO retina at P21 (figure 2j-m),
185 suggesting that the increased cell death that occurs in the ONL of the mutant mice after birth is
186 accompanied by the activation of glial cells.

187

188 **3.3. Inflammation-related gene expression is up-regulated in the *Prom1*-KO mouse retina**

189 We next sought to identify genes whose expression might be affected by *Prom1* deficiency by
190 subjecting the retina of WT and *Prom1*-KO mice at P14 and P21 to high-throughput expression analysis
191 based on RNA sequencing. Gene expression at P14 tended to vary within each genotype, and the only
192 gene whose expression differed significantly between genotypes was *Prom1* itself (figure 3a,
193 supplementary table S2), suggesting that *Prom1* does not significantly influence the gene expression

194 profile at P14. In contrast, the expression of various genes differed between the two genotypes at P21
195 (figure 3b, supplementary table S3). The expression of 1,081 and 766 genes was thus up- and down-
196 regulated, respectively, in the *Prom1*-KO retina with a *p* value of <0.01. In particular, expression of *Edn2*
197 was the most consistently and markedly up-regulated in the *Prom1*-KO retina. The expression of genes
198 associated with the inflammatory response - such as *Ifi44l*, *Serpina3n*, *S100a6*, *Bcl3*, and *Gfap* - was also
199 increased in the *Prom1*-KO retina at P21. Conversely, the expression of genes related to RP or of those
200 essential for retinal development and functional homeostasis - including *Fscn2* (RP30) [19], *Prph2* (RP7)
201 [20], *Nr2e3* (RP37) [21], *Kcnv2* [22], *Elovl2* [23], *Pde6b* (RD1) [24], and *Ttc21b* [25] - was down-
202 regulated in the *Prom1*-KO retina at P21 (supplementary table S3). GO term analysis revealed that several
203 signalling pathways, including apoptotic (TNF) and infectious-related signal (Epstein-Barr virus infection)
204 signals, were affected by the loss of *Prom1* (figure 3c).

205 We also investigated whether the observed effects of *Prom1* deficiency on gene expression were
206 specific to the retina. Given that *Prom1* is expressed in the retina, RPE, and testis [2], we performed RT-
207 qPCR analysis of RNA prepared from these tissues of WT and *Prom1*-KO mice at P21. Consistent, with
208 the results of our RNA-sequencing analysis, the expression of *Edn2*, *Bcl3*, and *Gfap* was increased in the
209 retina of *Prom1*-KO mice (figure 3d). However, the expression of these genes in the RPE and testis did
210 not differ between the two genotypes, indicating that the effect of *Prom1* on their expression is specific to
211 the retina. Together, these various data suggested that *Prom1* deficiency results in up-regulation of
212 inflammation-related genes and down-regulation of genes essential for functional homeostasis of
213 photoreceptor cells at 3 weeks after birth.

214

215 **3.4. Inflammation-related gene expression is increased by light stimulation in the *Prom1*-KO mouse** 216 **retina**

217 To determine the mechanism underlying the up-regulation of specific gene expression apparent in the
218 retina of *Prom1*-KO mice at P21, we examined whether light stimulation might play a role. We therefore
219 compared such gene expression between P21 retinas obtained from *Prom1*-KO mice reared under a
220 normal day-night cycle or in the dark. RT-qPCR analysis revealed that, whereas the expression of *Edn2*,
221 *Bcl3*, and *Gfap* did not differ between *Prom1*-KO and WT mice reared in the dark condition, marked up-
222 regulation of the expression of each of these genes was apparent specifically in *Prom1*-KO mice raised
223 under the normal day-night condition (figure 4a). Consistent with these results, immunofluorescence
224 analysis showed that the number of GFAP-positive cells in the retina was smaller for *Prom1*-KO mice
225 reared in the dark compared with those reared under the normal condition (figure 4b and c). To examine
226 further the effect of light on gene expression, we maintained *Prom1*-KO mice and their WT littermates
227 under the dark condition for 3 weeks, exposed them to a bright light for 3 h, and then allowed them to
228 recover for 3 days in the dark. The retina was then dissected and subjected to RT-qPCR and
229 immunofluorescence analyses. Light stimulation resulted in a marked increase both in the expression of
230 *Edn2* and *Bcl3* (Figure 4d) and in the number of GFAP-positive cells (figure 4e) in the retina of *Prom1*-

231 KO mice but not in that of WT mice. Collectively, these results thus suggested that the up-regulation of
232 *Edn2*, *Bcl3*, and *Gfap* expression apparent in the retina of *Prom1*-KO mice is an immediate response to
233 light stimulation, and that the inflammatory response mediated by these genes is one of the primary events
234 leading to degeneration of the mutant retina.

235

236 **3.5. Endothelin receptor antagonists attenuate *Gfap* expression and gliosis in the *Prom1*-KO mouse** 237 **retina**

238 Endothelin acts at specific receptors [26, 27] to increase both the number of GFAP-positive
239 Müller cells [28] and retinal cell death [29]. Given the elevated expression of *Edn2* and *Gfap* apparent in
240 the retina of *Prom1*-KO mice, we hypothesised that *Edn2* might induce aberrant proliferation of glial cells
241 and GFAP expression in association with retinal degeneration in these animals. We therefore examined
242 the possible effects of endothelin receptor antagonists in the mutant mice.

243 The drugs BQ-123 and BQ-788, which target endothelin receptors A and B, respectively [30],
244 were both injected intraperitoneally into *Prom1*-KO mice at P14, P19, and P24, and the mice were
245 analysed at P28. Whereas GFAP-positive cells were not observed in the retina of WT mice, they were
246 detected in that of *Prom1*-KO mice treated with dimethyl sulphoxide (DMSO) vehicle (figure 5a and b).
247 However, the number of GFAP-positive cells was markedly reduced in the mutant mice by treatment with
248 BQ-123 and BQ-788 (figure 5c). Staining of retinal flat-mount preparations with fluorescently labelled
249 isolectin to detect vascular endothelial cells also revealed fewer retinal vessels in *Prom1*-KO mice than in
250 WT mice and that this difference was attenuated by treatment of the mutant animals with BQ-123 and BQ-
251 788 (figure 5d–g).

252 RT-qPCR analysis showed that the expression of *Edn2*, *Bcl3*, and *Gfap* was increased in the retina
253 of *Prom1*-KO mice at P28 compared with that in WT mice. Whereas the expression of *Edn2* and *Bcl3* in
254 the mutant retina was not affected by treatment with BQ-123 and BQ-788, that of *Gfap* was significantly
255 attenuated (figure 5h), suggesting that up-regulation of *Gfap* expression in the mutant retina is mediated
256 by endothelin receptor signalling but that that of *Edn2* and *Bcl3* expression is not.

257 Finally, we examined the effect of BQ-123 and BQ-788 treatment on the number of apoptotic
258 cells in the retina of *Prom1*-KO mice. The TUNEL assay revealed that the marked increase in the number
259 of such cells apparent in the mutant retina at P28 was significantly attenuated by administration of the two
260 drugs (figure 5i), suggesting that endothelin receptor signalling contributes to loss of retinal cell
261 homeostasis.

262 4. Discussion

263 We have here described early manifestations of the retinal degeneration that occurs in *Prom1*-KO
264 mice and identified related genes. We thus detected the aberrant presence of glial cells and the expression
265 of genes associated with the inflammatory response in the mutant retina. Given that the expression of
266 these genes was not activated in the retina of *Prom1*-KO mice maintained in the dark condition, this
267 inflammatory response appears to be dependent on light stimulation. Finally, we found that the
268 deterioration and gliosis characteristic of the mutant retina were ameliorated by the administration of
269 endothelin receptor antagonists.

270 Although we found that *Prom1* is expressed in the retina from birth, the loss of *Prom1* did not
271 substantially affect the expression level of any gene in the retina at P14, suggesting that *Prom1* may not
272 play an essential role in the retina prior to light exposure. We previously showed by RT-qPCR analysis
273 that the expression of both *Rdh12* and *Abca4*, two genes that contribute to the visual cycle, was reduced in
274 the retina of *Prom1*-KO mice compared with that of WT mice at P14 [6], suggesting that impairment of
275 the visual cycle might lead to retinal degeneration. Although this result is reproducible as assayed by RT-
276 qPCR (supplementary figure S1), the difference in the expression level of each gene between the two
277 genotypes was associated with a relatively high *p* value in the high-throughput expression analysis
278 performed in the present study (figure 3, supplementary table 2), suggesting this decrease is not critical.

279 In contrast to the lack of an effect of *Prom1* deficiency on the gene expression profile of the retina
280 at P14, we detected many genes, including those related to the inflammatory response, as well as
281 signalling pathways whose activity was altered in the *Prom1*-KO retina at P21. The expression of genes
282 related to phototransduction, for example, was significantly down-regulated in the *Prom1*-KO retina at
283 P21 (figure 3c, supplementary table S3), indicating that *Prom1* may be essential for the transcription of
284 such genes or may form a transcriptional network with them. Of note, we found that the expression of
285 causal genes for RP was also down-regulated in the mutant retina at P21.

286 Of the genes whose expression was up-regulated in the *Prom1*-KO retina at P21, *Edn2* showed the
287 largest fold change. *Edn2* encodes a secretory peptide that plays a role in a wide range of biological
288 processes, including smooth muscle contraction and ovulation [31] as well as development of the enteric
289 nervous system [32]. Its expression is also induced in association with the inflammatory response and
290 promotes glial cell proliferation in the central nervous system [33]. Furthermore, consistent with the
291 perturbation of the retinal vasculature in *Prom1*-KO mice apparent in both the present and a previous [7]
292 study, *Edn2* has been found to inhibit retinal vascular development [34]. On the other hand, it was also
293 shown to promote photoreceptor cell survival [35]. These various observations suggest that the role of
294 *Edn2* in the photoreceptor degeneration associated with RP and MD is complex.

295 The expression of *Edn2* has also been shown to be up-regulated in other mouse models of RP [35],
296 including retina-specific *Cdhr1*-KO mice [36], with *Prom1* and *Cdhr1* having been found to interact with
297 each other [4]. In addition to *Edn2*, the other genes whose expression was affected in the *Prom1*-KO

298 mouse retina overlapped markedly with those affected in the conditional *Cdhr1*-KO mouse retina,
299 suggesting that *Prom1* and *Cdhr1* may function in the same intracellular signalling pathways.

300 Although we found that the expression of *Edn2* and *Bcl3* in the *Prom1*-KO retina was induced by
301 light stimulation, the mechanism underlying this effect remains unclear. Nevertheless, our study suggests
302 the possibility that an imbalance in intracellular ions caused by the loss of *Prom1* (given that *Prom1*
303 regulates chloride conductance activated by intracellular calcium uptake [12]) may impair the function of
304 cytoplasmic organelles such as mitochondria and the endoplasmic reticulum, and thereby elicit a stress
305 response. Studies to identify the transcriptional regulatory elements of *Edn2* and the corresponding
306 transcription factors and upstream signalling pathways underlying its photoactivation are warranted.

307 Gliosis is a response to injury in the central nervous system and is associated with the appearance
308 of GFAP-positive glial cells [26]. It is also a feature of certain neurodegenerative retinal diseases
309 including RP [37], with gliosis in RP having been found to be related to several RP genes. Targeting of
310 gliosis is therefore a potential clinical strategy to delay disease progression and ameliorate associated
311 symptoms. We have now shown that administration of endothelin receptor antagonists attenuated both the
312 appearance of GFAP-positive glial cells and vascular endothelial constriction in the retina of *Prom1*-KO
313 mice. These findings indicate that blockade of endothelin signalling may be an effective clinical strategy
314 for the treatment of gliosis. However, caution is warranted with such an approach for the treatment of RP,
315 given the various functions of endothelins and the consequent potential for adverse systemic effects.
316 Intravitreal injection of endothelin receptor antagonists may help to avoid such side effects. Gene therapy
317 targeting endothelin receptor function is also a potential therapeutic approach for RP. Finally, replacement
318 of dead tissue with functional cells through a regenerative medicine approach may be required for the
319 successful treatment of RP and MD [38].

320 In conclusion, our results implicating up-regulation of *Edn2* expression in the retinal pathology of
321 *Prom1*-KO mice suggest that localized pharmacological targeting of endothelin receptor signalling
322 warrants further investigation as a clinical intervention for the prevention or treatment of retinal
323 degenerative diseases such as RP and MD.

324 **Ethics.** All animal experiments were approved by the animal welfare and ethics committees of both
325 Yamaguchi University (approval numbers J16021 and U16005 for K.K.) and Nara Institute of Science and
326 Technology (approval numbers 1810 and 311 for N.S.) and were performed in accordance with the
327 relevant guidelines and regulations.

328

329 **Data availability.** Data are available in the main text/figures and in the Supplementary Information.

330

331 **Competing interests.** The authors declare no competing interests.

332

333 **Funding.** This work was supported in part by grants-in-aid for scientific research from Japan Society for
334 the Promotion of Science (17H03684 and 20H0326310 to N.S.; 20K09805 to K.K.), as well as by
335 Novartis Pharma.

336

337 **Acknowledgements.** We thank Erika Yoshihara, Yukari Mizuno, and Ayaka Kataoka for technical
338 assistance as well as other laboratory members for their support and discussion.

339

340 **Author Contributions.** KK and NS conceived the project; YK, NS, SW, MS, CY, TO, FH, TY
341 performed experiments; YK, NS, MS, TH, YA analysed the data; All authors joined the discussion; NS,
342 KK, YK wrote the manuscript.

343 References

- 344 1 Ferrari, S., Di Iorio, E., Barbaro, V., Ponzin, D., Sorrentino, F. S., Parmeggiani, F. 2011 Retinitis
345 pigmentosa: genes and disease mechanisms. *Curr Genomics*. **12**, 238-249.
346 (10.2174/138920211795860107)
- 347 2 Fargeas, C. A., Joester, A., Missol-Kolka, E., Hellwig, A., Huttner, W. B., Corbeil, D. 2004
348 Identification of novel Prominin-1/CD133 splice variants with alternative C-termini and their
349 expression in epididymis and testis. *Journal of cell science*. **117**, 4301-4311. (10.1242/jcs.01315)
- 350 3 Maw, M. A., Corbeil, D., Koch, J., Hellwig, A., Wilson-Wheeler, J. C., Bridges, R. J.,
351 Kumaramanickavel, G., John, S., Nancarrow, D., Roper, K., *et al.* 2000 A frameshift mutation in
352 prominin (mouse)-like 1 causes human retinal degeneration. *Human molecular genetics*. **9**, 27-34.
- 353 4 Yang, Z., Chen, Y., Lillo, C., Chien, J., Yu, Z., Michaelides, M., Klein, M., Howes, K. A., Li, Y.,
354 Kaminoh, Y., *et al.* 2008 Mutant prominin 1 found in patients with macular degeneration disrupts
355 photoreceptor disk morphogenesis in mice. *The Journal of clinical investigation*. **118**, 2908-2916.
356 (10.1172/JCI35891)
- 357 5 Michaelides, M., Gaillard, M. C., Escher, P., Tiab, L., Bedell, M., Borruat, F. X., Barthelmes, D.,
358 Carmona, R., Zhang, K., White, E., *et al.* 2010 The PROM1 mutation p.R373C causes an autosomal
359 dominant bull's eye maculopathy associated with rod, rod-cone, and macular dystrophy. *Investigative
360 ophthalmology & visual science*. **51**, 4771-4780. (10.1167/iovs.09-4561)
- 361 6 Dellett, M., Sasai, N., Nishide, K., Becker, S., Papadaki, V., Limb, G. A., Moore, A. T., Kondo, T.,
362 Ohnuma, S. 2015 Genetic background and light-dependent progression of photoreceptor cell
363 degeneration in Prominin-1 knockout mice. *Investigative ophthalmology & visual science*. **56**, 164-176.
364 (10.1167/iovs.14-15479)
- 365 7 Zacchigna, S., Oh, H., Wilsch-Brauninger, M., Missol-Kolka, E., Jaszai, J., Jansen, S., Tanimoto, N.,
366 Tonagel, F., Seeliger, M., Huttner, W. B., *et al.* 2009 Loss of the cholesterol-binding protein prominin-
367 1/CD133 causes disk dysmorphogenesis and photoreceptor degeneration. *The Journal of
368 neuroscience : the official journal of the Society for Neuroscience*. **29**, 2297-2308.
369 (10.1523/JNEUROSCI.2034-08.2009)
- 370 8 Boivin, D., Labbe, D., Fontaine, N., Lamy, S., Beaulieu, E., Gingras, D., Beliveau, R. 2009 The stem
371 cell marker CD133 (prominin-1) is phosphorylated on cytoplasmic tyrosine-828 and tyrosine-852 by
372 Src and Fyn tyrosine kinases. *Biochemistry*. **48**, 3998-4007. (10.1021/bi900159d)
- 373 9 Wei, Y., Jiang, Y., Zou, F., Liu, Y., Wang, S., Xu, N., Xu, W., Cui, C., Xing, Y., Liu, Y., *et al.* 2013
374 Activation of PI3K/Akt pathway by CD133-p85 interaction promotes tumorigenic capacity of glioma
375 stem cells. *Proceedings of the National Academy of Sciences of the United States of America*. **110**,
376 6829-6834. (10.1073/pnas.1217002110)
- 377 10 Khatri, P., Obernier, K., Simeonova, I. K., Hellwig, A., Holzl-Wenig, G., Mandl, C., Scholl, C., Wolf,
378 S., Winkler, J., Gaspar, J. A., *et al.* 2014 Proliferation and cilia dynamics in neural stem cells
379 prospectively isolated from the SEZ. *Scientific reports*. **4**, 3803. (10.1038/srep03803)
- 380 11 Singer, D., Thamm, K., Zhuang, H., Karbanova, J., Gao, Y., Walker, J. V., Jin, H., Wu, X., Coveney, C.
381 R., Marangoni, P., *et al.* 2019 Prominin-1 controls stem cell activation by orchestrating ciliary
382 dynamics. *The EMBO journal*. **38**, (10.15252/embj.201899845)
- 383 12 Hori, A., Nishide, K., Yasukuni, Y., Haga, K., Kakuta, W., Ishikawa, Y., Hayes, M. J., Ohnuma, S. I.,
384 Kiyonari, H., Kimura, K., *et al.* 2019 Prominin-1 Modulates Rho/ROCK-Mediated Membrane
385 Morphology and Calcium-Dependent Intracellular Chloride Flux. *Scientific reports*. **9**, 15911.
386 (10.1038/s41598-019-52040-9)
- 387 13 Robinson, M. D., McCarthy, D. J., Smyth, G. K. 2010 edgeR: a Bioconductor package for differential
388 expression analysis of digital gene expression data. *Bioinformatics*. **26**, 139-140.
389 (10.1093/bioinformatics/btp616)
- 390 14 Yamaguchi, M., Nakao, S., Arita, R., Kaizu, Y., Arima, M., Zhou, Y., Kita, T., Yoshida, S., Kimura,
391 K., Isobe, T., *et al.* 2016 Vascular Normalization by ROCK Inhibitor: Therapeutic Potential of
392 Ripasudil (K-115) Eye Drop in Retinal Angiogenesis and Hypoxia. *Investigative ophthalmology &
393 visual science*. **57**, 2264-2276. (10.1167/iovs.15-17411)
- 394 15 Chang, M. L., Wu, C. H., Jiang-Shieh, Y. F., Shieh, J. Y., Wen, C. Y. 2007 Reactive changes of retinal
395 astrocytes and Muller glial cells in kainate-induced neuroexcitotoxicity. *J Anat*. **210**, 54-65.
396 (10.1111/j.1469-7580.2006.00671.x)

- 397 16 Lewis, G. P., Fisher, S. K. 2003 Up-regulation of glial fibrillary acidic protein in response to retinal
398 injury: its potential role in glial remodeling and a comparison to vimentin expression. *Int Rev Cytol.*
399 **230**, 263-290. (10.1016/s0074-7696(03)30005-1)
- 400 17 Rojas, B., Gallego, B. I., Ramirez, A. I., Salazar, J. J., de Hoz, R., Valiente-Soriano, F. J., Aviles-
401 Trigueros, M., Villegas-Perez, M. P., Vidal-Sanz, M., Trivino, A., *et al.* 2014 Microglia in mouse
402 retina contralateral to experimental glaucoma exhibit multiple signs of activation in all retinal layers. *J*
403 *Neuroinflammation*. **11**, 133. (10.1186/1742-2094-11-133)
- 404 18 Omri, S., Behar-Cohen, F., de Kozak, Y., Sennlaub, F., Verissimo, L. M., Jonet, L., Savoldelli, M.,
405 Omri, B., Crisanti, P. 2011 Microglia/macrophages migrate through retinal epithelium barrier by a
406 transcellular route in diabetic retinopathy: role of PKCzeta in the Goto Kakizaki rat model. *Am J*
407 *Pathol.* **179**, 942-953. (10.1016/j.ajpath.2011.04.018)
- 408 19 Wada, Y., Abe, T., Takeshita, T., Sato, H., Yanashima, K., Tamai, M. 2001 Mutation of human retinal
409 fascin gene (FSCN2) causes autosomal dominant retinitis pigmentosa. *Investigative ophthalmology &*
410 *visual science*. **42**, 2395-2400.
- 411 20 Conley, S. M., Naash, M. I. 2014 Gene therapy for PRPH2-associated ocular disease: challenges and
412 prospects. *Cold Spring Harbor perspectives in medicine*. **4**, a017376. (10.1101/cshperspect.a017376)
- 413 21 Cheng, H., Khanna, H., Oh, E. C., Hicks, D., Mitton, K. P., Swaroop, A. 2004 Photoreceptor-specific
414 nuclear receptor NR2E3 functions as a transcriptional activator in rod photoreceptors. *Human*
415 *molecular genetics*. **13**, 1563-1575. (10.1093/hmg/ddh173)
- 416 22 Holter, P., Kunst, S., Wolloscheck, T., Kelleher, D. K., Sticht, C., Wolfrum, U., Spessert, R. 2012 The
417 retinal clock drives the expression of Kcnv2, a channel essential for visual function and cone survival.
418 *Investigative ophthalmology & visual science*. **53**, 6947-6954. (10.1167/iovs.12-10234)
- 419 23 Chen, D., Chao, D. L., Rocha, L., Kolar, M., Nguyen Huu, V. A., Krawczyk, M., Dasyani, M., Wang,
420 T., Jafari, M., Jabari, M., *et al.* 2020 The lipid elongation enzyme ELOVL2 is a molecular regulator of
421 aging in the retina. *Aging Cell*. **19**, e13100. (10.1111/ace1.13100)
- 422 24 Yeo, J. H., Jung, B. K., Lee, H., Baek, I. J., Sung, Y. H., Shin, H. S., Kim, H. K., Seo, K. Y., Lee, J. Y.
423 2019 Development of a Pde6b Gene Knockout Rat Model for Studies of Degenerative Retinal Diseases.
424 *Investigative ophthalmology & visual science*. **60**, 1519-1526. (10.1167/iovs.18-25556)
- 425 25 Liu, Q., Zhang, Q., Pierce, E. A. 2010 Photoreceptor sensory cilia and inherited retinal degeneration.
426 *Advances in experimental medicine and biology*. **664**, 223-232. (10.1007/978-1-4419-1399-9_26)
- 427 26 Sarthy, V. P., Sawkar, H., Dudley, V. J. 2015 Endothelin2 Induces Expression of Genes Associated
428 with Reactive Gliosis in Retinal Muller Cells. *Curr Eye Res.* **40**, 1181-1184.
429 (10.3109/02713683.2014.982828)
- 430 27 Patel, C., Narayanan, S. P., Zhang, W., Xu, Z., Sukumari-Ramesh, S., Dhandapani, K. M., Caldwell, R.
431 W., Caldwell, R. B. 2014 Activation of the endothelin system mediates pathological angiogenesis
432 during ischemic retinopathy. *Am J Pathol.* **184**, 3040-3051. (10.1016/j.ajpath.2014.07.012)
- 433 28 Rattner, A., Toulabi, L., Williams, J., Yu, H., Nathans, J. 2008 The genomic response of the retinal
434 pigment epithelium to light damage and retinal detachment. *The Journal of neuroscience : the official*
435 *journal of the Society for Neuroscience*. **28**, 9880-9889. (10.1523/JNEUROSCI.2401-08.2008)
- 436 29 Kobayashi, T., Oku, H., Fukuhara, M., Kojima, S., Komori, A., Ichikawa, M., Katsumura, K.,
437 Kobayashi, M., Sugiyama, T., Ikeda, T. 2005 Endothelin-1 enhances glutamate-induced retinal cell
438 death, possibly through ETA receptors. *Investigative ophthalmology & visual science*. **46**, 4684-4690.
439 (10.1167/iovs.05-0785)
- 440 30 Fukuroda, T., Ozaki, S., Ihara, M., Ishikawa, K., Yano, M., Nishikibe, M. 1994 Synergistic inhibition
441 by BQ-123 and BQ-788 of endothelin-1-induced contractions of the rabbit pulmonary artery. *Br J*
442 *Pharmacol.* **113**, 336-338. (10.1111/j.1476-5381.1994.tb16901.x)
- 443 31 Cacioppo, J. A., Oh, S. W., Kim, H. Y., Cho, J., Lin, P. C., Yanagisawa, M., Ko, C. 2014 Loss of
444 function of endothelin-2 leads to reduced ovulation and CL formation. *PloS one*. **9**, e96115.
445 (10.1371/journal.pone.0096115)
- 446 32 Gershon, M. D. 1999 Endothelin and the development of the enteric nervous system. *Clin Exp*
447 *Pharmacol Physiol.* **26**, 985-988. (10.1046/j.1440-1681.1999.03176.x)
- 448 33 Yuen, T. J., Johnson, K. R., Miron, V. E., Zhao, C., Quandt, J., Harrisingh, M. C., Swire, M., Williams,
449 A., McFarland, H. F., Franklin, R. J., *et al.* 2013 Identification of endothelin 2 as an inflammatory
450 factor that promotes central nervous system remyelination. *Brain*. **136**, 1035-1047.
451 (10.1093/brain/awt024)

- 452 34 Rattner, A., Yu, H., Williams, J., Smallwood, P. M., Nathans, J. 2013 Endothelin-2 signaling in the
453 neural retina promotes the endothelial tip cell state and inhibits angiogenesis. *Proceedings of the*
454 *National Academy of Sciences of the United States of America*. **110**, E3830-3839.
455 (10.1073/pnas.1315509110)
- 456 35 Bramall, A. N., Szego, M. J., Pacione, L. R., Chang, I., Diez, E., D'Orleans-Juste, P., Stewart, D. J.,
457 Hauswirth, W. W., Yanagisawa, M., McInnes, R. R. 2013 Endothelin-2-mediated protection of mutant
458 photoreceptors in inherited photoreceptor degeneration. *PloS one*. **8**, e58023.
459 (10.1371/journal.pone.0058023)
- 460 36 Rattner, A., Nathans, J. 2005 The genomic response to retinal disease and injury: evidence for
461 endothelin signaling from photoreceptors to glia. *The Journal of neuroscience : the official journal of*
462 *the Society for Neuroscience*. **25**, 4540-4549. (10.1523/JNEUROSCI.0492-05.2005)
- 463 37 Roche, S. L., Ruiz-Lopez, A. M., Moloney, J. N., Byrne, A. M., Cotter, T. G. 2018 Microglial-induced
464 Muller cell gliosis is attenuated by progesterone in a mouse model of retinitis pigmentosa. *Glia*. **66**,
465 295-310. (10.1002/glia.23243)
- 466 38 Stern, J. H., Tian, Y., Funderburgh, J., Pellegrini, G., Zhang, K., Goldberg, J. L., Ali, R. R., Young, M.,
467 Xie, Y., Temple, S. 2018 Regenerating Eye Tissues to Preserve and Restore Vision. *Cell Stem Cell*. **22**,
468 834-849. (10.1016/j.stem.2018.05.013)
- 469

470 **Figure Legends**

471 **Figure 1.** *Prom1* is expressed in the ONL of the retina from perinatal to adult stages. The retina of
472 heterozygous *Prom1* mutant mice at P2 (*a-a''*), P14, (*b-b''*), P21 (*c-c''*), and P42 (*d-d''*) was subjected to
473 staining of β -gal activity (*a,b,c,d*) as well as to staining of nuclei with DAPI (*a',b',c',d'*). Merged images
474 are also shown (*a'',b'',c'',d''*). Data are representative of three retinas at each age. Scale bar in (*a*) is (50
475 μ m) and applies to all images. RPE, retinal pigment epithelium; NBL, neuroblast layer; GCL, ganglion
476 cell layer; OS, outer segments; IS, inner segments; ONL, outer nuclear layer; OPL, outer plexiform layer;
477 INL, inner nuclear layer; IPL, inner plexiform layer.

478
479 **Figure 2.** Programmed cell death and an inflammatory response in the postnatal *Prom1*-KO mouse retina.
480 (*a-d''*) TUNEL staining of the WT (*a-a''*,*c-c''*) and *Prom1*-KO (*b-b''*,*d-d''*) mouse retina at P14 (*a-b''*)
481 and P21 (*c-d''*). Nuclei were stained with DAPI (*a',b',c',d'*). Merged images of TUNEL (red) and DAPI
482 (blue) staining are also shown (*a'',b'',c'',d''*). Arrowheads in (*d,d''*) indicate apoptotic cells. (*e*)
483 Quantitation of the proportion of TUNEL-positive cells among all DAPI-stained cells for images similar
484 to those in (*a*),(*b*),(*c*) and (*d*). Data are means \pm s.e.m. for four retinas for each condition. ** $p < 0.01$; n.s.,
485 not significant (two-tailed Student's *t* test). (*f-m*) Immunofluorescence staining for GFAP (*f, h,j,l*) and Iba-
486 1 (*g,i,k,m*) in the retina of WT (*f,g,j,k*) and *Prom1*-KO (*h,i,l,m*) mice at P14 (*f-i*) and P21 (*j-m*). Merged
487 images with DAPI staining are also shown (*f',g',h',i',j',k',l',m'*). Arrowheads in (*m*) indicate Iba-1-
488 positive cells. Data are representative of three (P14) or five (P21) retinas for each genotype. Scale bar in
489 (*a*) is 50 μ m and applies to all images.

490
491 **Figure 3.** Effects of *Prom1* deficiency on gene expression in the retina. (*a,b*) Volcano plots for RNA-
492 sequencing analysis of the retina of *Prom1*-KO mice relative to that of WT mice at P14 (*a*) and P21 (*b*).
493 Genes with a p value of 1×10^{-10} are indicated with the blue arrowhead in (*b*). A cut-off p value of 1×10^{-2}
494 is indicated by the green dashed line. Data are for three (P14) or four (P21) retinas of each genotype. (*c*)
495 GO term analysis based on KEGG pathways for genes whose expression differed significantly between
496 the retinas of *Prom1*-KO and WT mice in the RNA-sequencing analysis at P21. (*d*) RT-qPCR analysis of
497 *Edn2*, *Bcl3*, and *Gfap* expression in the retina, RPE, and testis of WT and *Prom1*-KO mice at P21. Data
498 are means \pm s.e.m. for three retinas of each genotype. * $p < 0.05$, ** $p < 0.01$, n.s., not significant (two-
499 tailed Student's *t* test).

500
501 **Figure 4.** Genes whose expression is increased by *Prom1* deficiency are up-regulated by light stimulation.
502 (*a*) RT-qPCR analysis of *Edn2*, *Bcl3*, and *Gfap* expression in the P21 retina of WT or *Prom1*-KO mice
503 that had been reared either under a normal day-night cycle or in the dark. Data are means \pm s.e.m. for four
504 retinas for each condition. * $p < 0.05$, ** $p < 0.01$, n.s., not significant, versus WT/normal (one-way
505 ANOVA followed by Tukey's post hoc test). (*b* and *c*) Immunofluorescence analysis of GFAP expression
506 in the retina of *Prom1*-KO mice raised as in (*a*). Merged images with DAPI staining are also shown. Scale

507 bar in (b) is 50 μm and applies to all images. Data are representative of four (dark) or seven (normal day-
508 night) retinas. (d) RT-qPCR analysis of *Edn2* and *Bcl3* expression in the retina of *Prom1*-KO and WT
509 mice that had been reared in the dark condition for 3 weeks, exposed (or not) to a bright light for 3 h, and
510 then allowed to recover in the dark for 3 days. Data are means \pm s.e.m. for five retinas for each condition.
511 * $p < 0.05$, n.s., not significant, versus WT/dark (one-way ANOVA followed by Tukey's post hoc test). (e)
512 Immunofluorescence analysis of GFAP expression in the retina of *Prom1*-KO mice raised in the dark and
513 stimulated with light as in (d). Merged images with DAPI staining are also shown. Data are representative
514 of three retinas.

515

516 **Figure 5.** Endothelin receptor antagonists attenuate the increase in the number of GFAP-positive cells and
517 vascular stenosis in the retina of *Prom1*-KO mice. (a–c) Immunofluorescence analysis of GFAP
518 expression in the retina of WT (a) or *Prom1*-KO (b and c) mice treated with the combination of BQ-123
519 and BQ-788 (c) or with DMSO vehicle (a and b) at P14, P19, and P24 and analysed at P28. Merged
520 images with DAPI staining are also shown. Scale bar in (a), 50 μm . Data are representative of three retinas
521 per condition. (d–f) Isolectin staining of the retina of mice as in (a) to (c). The boxed regions of the left
522 panels are shown at higher magnification in the right panels. Scale bars, 100 μm . (g) Area of blood vessels
523 measured in images similar to those in (d) to (f). Data are means + s.e.m. for X retinas per condition. * $p <$
524 0.05, **** $p < 0.0001$ (one-way ANOVA followed by Tukey's post hoc test). (h) RT-qPCR analysis of
525 *Edn2*, *Bcl3*, and *Gfap* expression in the retina of the treated mice. Data are means \pm s.e.m. for three retinas
526 per condition. ** $p < 0.01$, n.s., not significant (one-way ANOVA followed by Tukey's post hoc test). (i–k)
527 TUNEL staining for apoptotic cells in the retina of the treated mice. Merged images with DAPI staining
528 are also shown. Scale bar in (i), 50 μm . (l) Number of apoptotic cells determined from images similar to
529 those in (i) to (k). Data are means \pm s.e.m. for three retinas per condition. ** $p < 0.01$, *** $p < 0.001$ (one-
530 way ANOVA followed by Tukey's post hoc test).

531

532 **Supplementary Figure**

533 **Supplementary figure S1.** Expression of *Rdh12* and *Abca4* is down-regulated in the retina of *Prom1*-KO
534 mice at P14.

535

536 **Supplementary Tables**

537 **Supplementary table S1.** Primers used for this study.

538 **Supplementary table S2.** RNA-sequencing analysis of the retina of *Prom1*-KO and WT mice at P14.

539 **Supplementary table S3.** RNA-sequencing analysis of the retina of *Prom1*-KO and WT mice at P21.

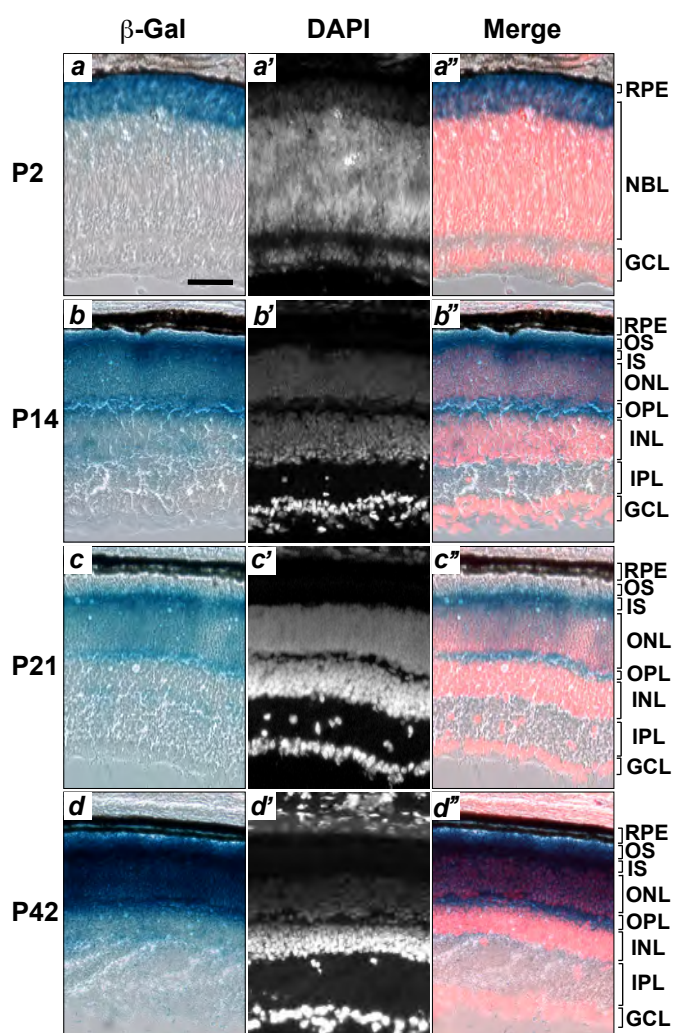


Figure 1

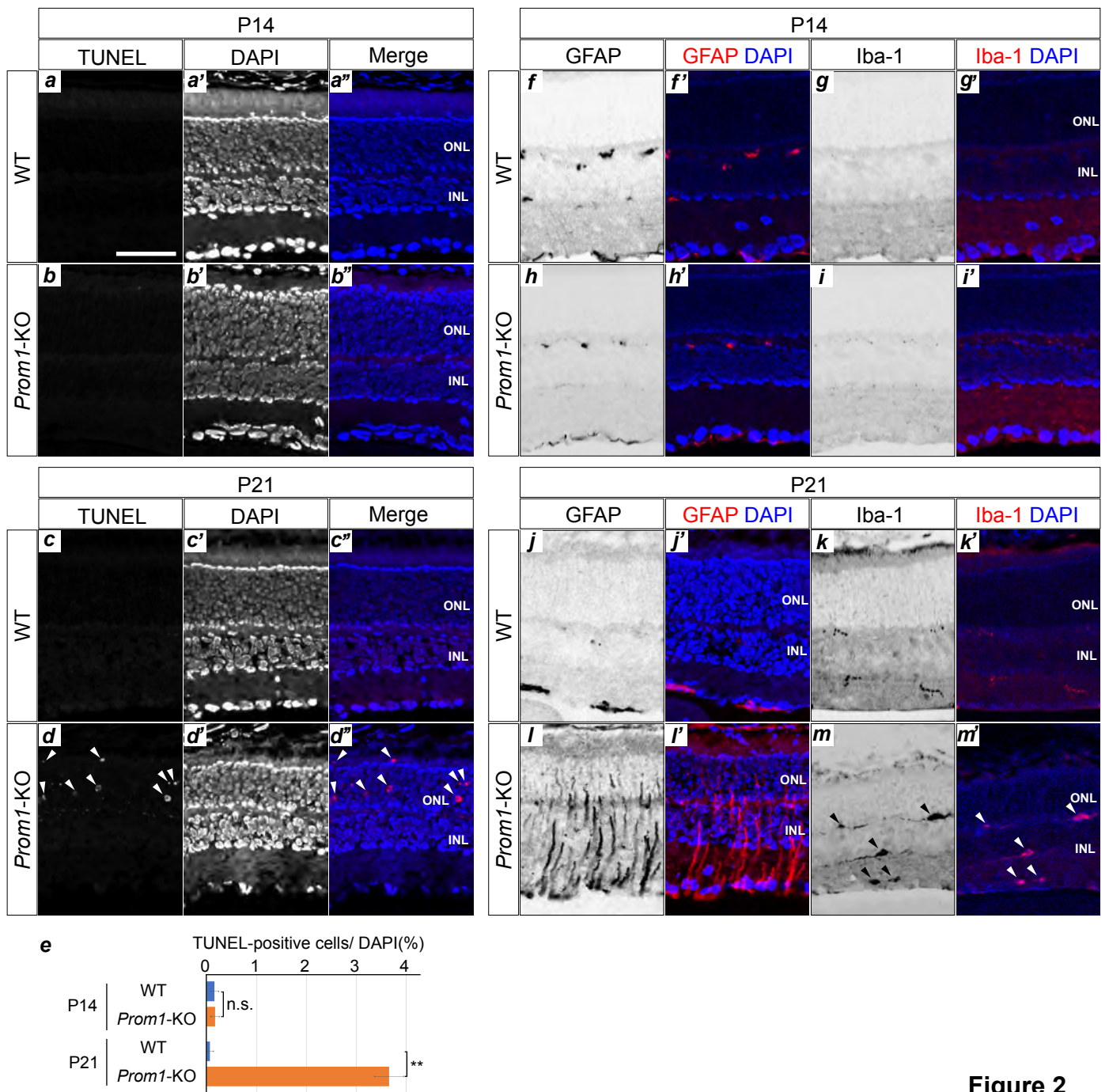


Figure 2

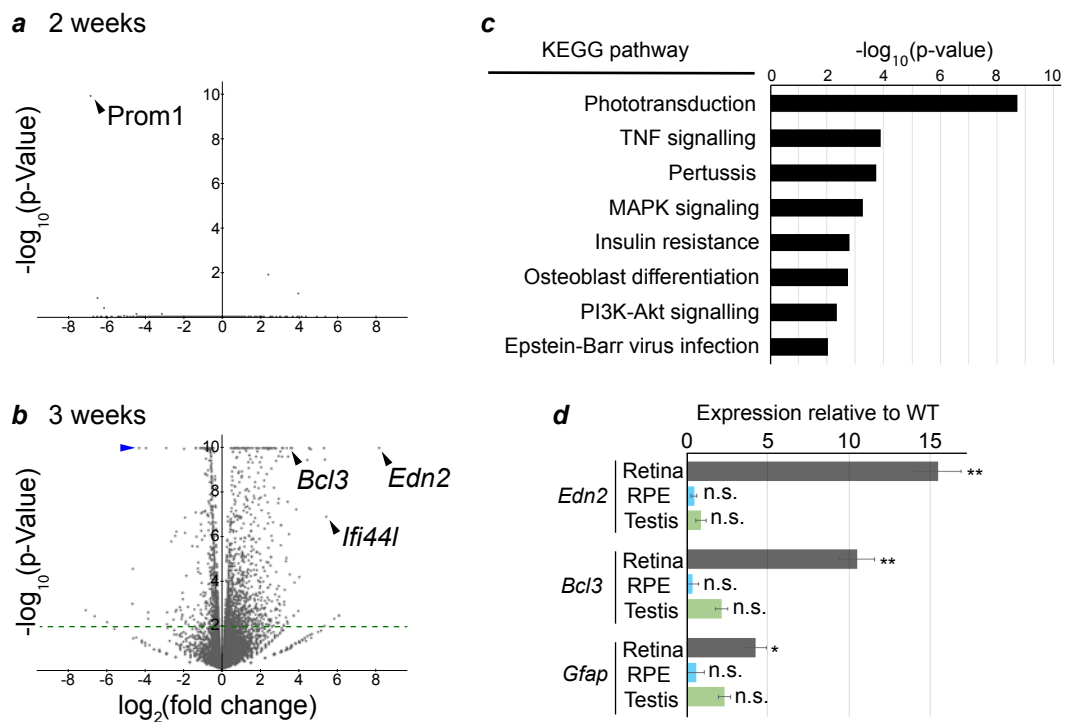


Figure 3

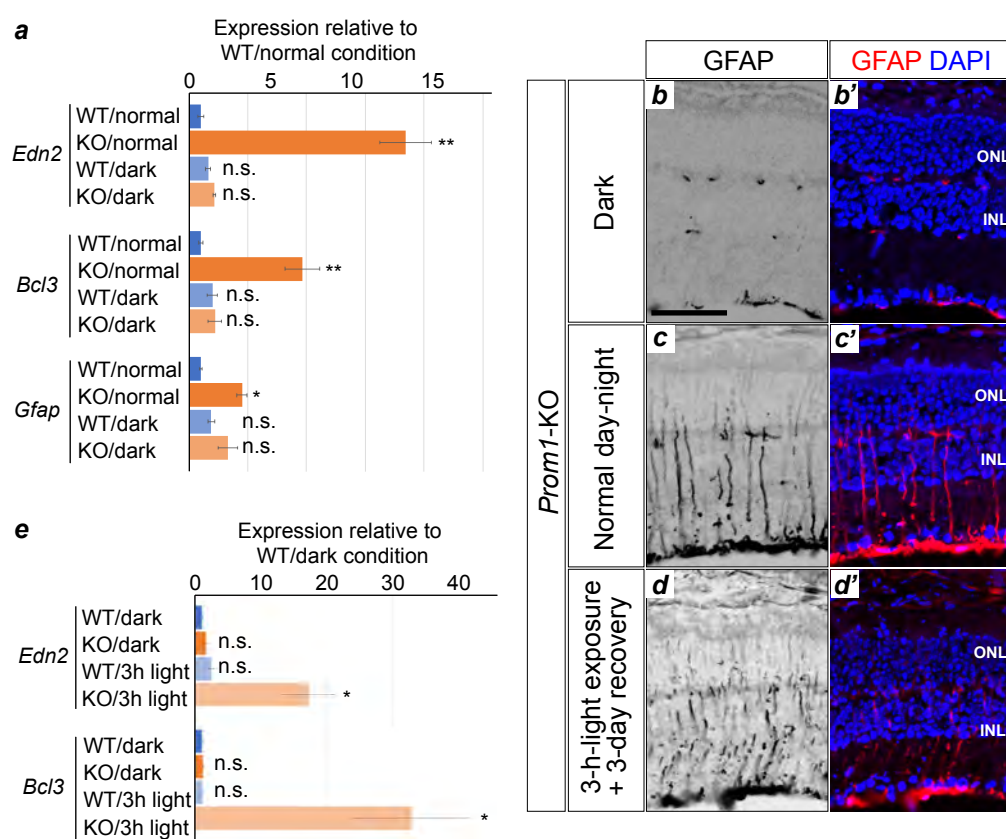


Figure 4

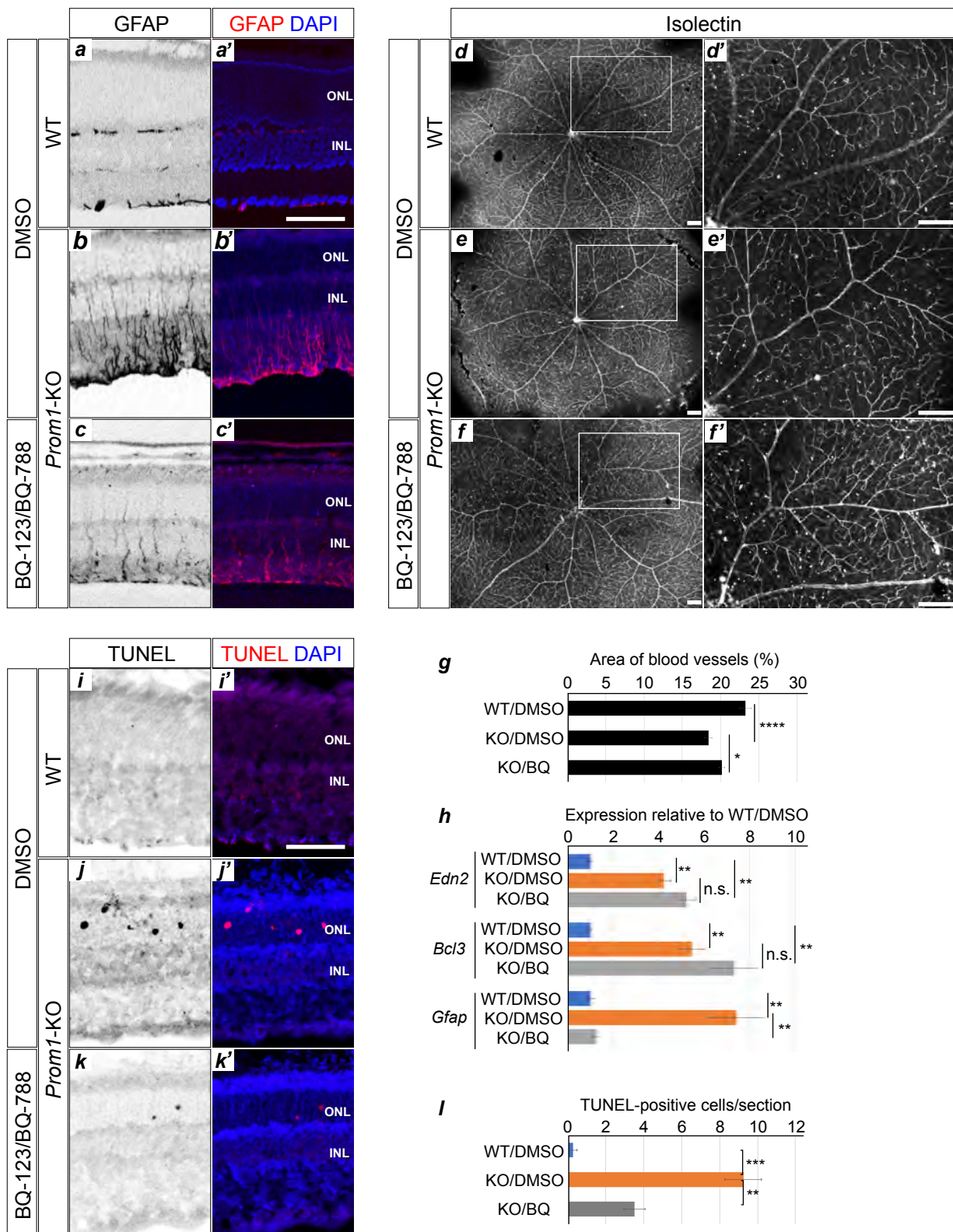


Figure 5